Comparison of the Isothermal Oxidation Behavior of As-Cast Cu-17%Cr and Cu-17%Cr-5%Al Part I: Oxidation Kinetics

S. V. Raj[#],

NASA Glenn Research Center, MS 106-5, 21000 Brookpark Road, Cleveland, OH 44135

ABSTRACT

The isothermal oxidation kinetics of as-cast Cu-17%Cr and Cu-17%Cr-5%Al in air were studied between 773 and 1173 K under atmospheric pressure. These observations reveal that Cu-17%Cr-5%Al oxidizes at significantly slower rates than Cu-17%Cr. The rate constants for the alloys were determined from generalized analyses of the data without an *a priori* assumption of the nature of the oxidation kinetics. Detailed analyses of the isothermal thermogravimetric weight change data revealed that Cu-17%Cr exhibited parabolic oxidation kinetics with an activation energy of 165.9 ± 9.5 kJ mol^{-1}. In contrast, the oxidation kinetics for the Cu-17%Cr-5%Al alloy exhibited a parabolic oxidation kinetics during the initial stages followed by a quartic relationship in the later stages of oxidation. Alternatively, the oxidation behavior of Cu-17%CR-5%Al could be better represented by a logarithmic relationship. The parabolic rate constants and activation energy data for the two alloys are compared with literature data to gain insights on the nature of the oxidation mechanisms dominant in these alloys.

Keywords

Isothermal oxidation; Cu-Cr alloys; Cu-Cr-Al; copper alloys; oxidation kinetics;

Tel.: (216) 433-8195; Fax: (216) 433-5544; e-mail: sai.v.raj@nasa.gov

1. Introduction

Uncoated copper alloy combustor liners are used extensively in rocket engines primarily due to their high thermal conductivity and suitable mechanical properties [1,2]. However, many of these commercial copper alloys are prone to extensive oxidation at temperatures exceeding 673 K [3]. Environmental damage of uncoated copper alloy liners, termed "blanching", is observed in a liquid hydrogen (LH_2) and liquid oxygen (LOX) rocket engine due to repeated oxidation-reduction cycles of the copper matrix [2]. As a result, the initially highly polished liner surface becomes very rough leading to degradation in the heat transfer characteristics of the engine. Repeated polishing of the liner surface of a reusable launch vehicle (RLV) after each mission cycle results in a corresponding decrease in the cross-sectional area of the cooling channels with a decreased ability to carry the mechanical stresses. Thus, it is clear that a fundamental understanding of the oxidation behavior of copper and its alloys being considered for use in rocket engines either as combustion liners or as coatings is desirable.

The oxidation of pure copper has been extensively studied by several investigators since the 1930's [3,4,5,6,7,8,9,10,11,12 ,13,14,15,16,17,18,19, 20,21,22]. These studies have elucidated the oxidation rate kinetics for copper [6,7,8,10,14,15,16,19,22] while largely confirming the applicability of the Wagner's parabolic oxidation rate theory for this metal above 473 K [14,15]. More recent studies have focused on the effect of a second phase on the oxidation kinetics of an almost pure Cu matrix [20,21,23,24,25]. In this regard, the Cu-Cr system has proved to be a model alloy system for these types of studies owing to the limited solubility of Cr in Cu [26,27]. Several studies have demonstrated that Cu-Cr alloys generally exhibit parabolic

oxidation kinetics although the compositions of the oxide scales appeared to depend on how the alloys were processed [20,21] and their grain size [20,21,23,25]. Although copper oxides have been reported in the surface scales after isothermal oxidation in these investigations, there is less commonality in the observed results as to whether these alloys form a protective chromia subsurface layer. This lack of consistency in the formation of a protective Cr_2O_3 is presumably due to variations in composition, alloy processing and microstructures.

Although Cu-17%Cr[i] [25] and Cu-Cr alloys with Cr ≥ 26% [28,29,30] have been proposed as protective coatings for copper alloy rocket engine combustion liners, there is an inherent danger in relying on alloys which do not consistently form a continuous protective Cr_2O_3 scales as coatings. Moreover, in developing coatings for copper alloy liners, it is especially important that the coating be deposited by a commercially viable processing method, such as a thermal spray technique, to reduce cost. Recent studies have demonstrated that vacuum plasma sprayed Cu-26%Cr overlay coated GRCop-84 (Cu-8at.%Cr-4%Nb) copper alloy substrates form blisters in a high heat flux H_2/O_2 combustion flame [31]. Further research has shown that while the oxidation resistance of the Cu-Cr alloys increase with increasing Cr content, their oxidation behavior remains essentially identical when 40% ≤ Cr ≤ 55% [32].

Early research by Nishimura [5] has demonstrated that the oxidation resistance of Cu-Al alloys improves significantly with increasing Al content with the oxidation of Cu-Al being relatively insignificant when the Al content increases above 5%. Later research on Cu-Al alloys also confirmed these early observations [33,34,35,36,37,38,39,40]. Limited data published by

[i] All compositions reported in this paper are in wt.% unless otherwise noted.

Nishimura [5] on Cu-0.25-1.0%Cr-8-10%Al alloys showed that the oxidation resistance of these alloys, while excellent, was essentially independent of Al content.

Based on Nishimura's early research [5], it is intriguing to pose the question: How will Al addition to Cu-Cr alloys change its oxidation behavior? It has been shown that Al and Cr act synergistically in MCrAl coatings, where M is either Co, Fe or Ni, resulting in the formation of a continuous, thermodynamically stable, protective Al_2O_3 external scale at lower values of Al of 5% than in binary M-Al alloys, where Al $\geq$ 17% for the formation of the alumina scale [41]. Unlike the MCrAl alloys, where both Al and Cr are in solid solution to a significant extent in the Co, Fe or Ni matrix, the binary phase Cu-Cr and Cu-Al phase diagrams suggest that there is comparatively small dissolution of Cr in Cu while Al dissolves up to 10% in Cu [27]. Similarly, the Cu-Cr-Al ternary phase diagram shows that the solubility of Al in the α-Cr and α-Cu phases is relatively small in Cu-Cr-Al alloys containing smaller amounts of Al but increases with increasing Al content in the two phase α-Cr/α-Cu region [42,43]. This raises the question as to whether the observed synergism between Al and Cr in the MCrAl alloys in forming a protective alumina scale is also applicable to the Cu-Cr-Al system. Recently, Niu *et al*. [44,45] conducted limited studies on the oxidation behavior of Cu-2 to 4(at.%)Al and Cu-4 to 8(at.%)Cr-2 to 4%Al alloys at 1073 K and reported the formation of an outer CuO external scale and an Al_2O_3 scale at the interface with the unoxidized matrix with a mixture of CuO and $(Cr,Al)_2O_3$ transition subsurface layer lying in between the external and innermost scales. It was observed that the continuity of the subsurface Al_2O_3 alumina scale depended on the amount of Cr present in the alloy although it was observed in all the Cr containing alloys. A major problem with this and other studies is that the time for oxidation was typically 24 h, which maybe too short to establish

steady-state oxidation behavior. Recently, it has been demonstrated that a Cu-23%Cr-5%Al coating developed for rocket engine applications provided excellent protection to the Cu-8at.%Cr-4%Nb copper alloy substrate.

The present two part paper compares the oxidation behavior of as-cast Cu-17%Cr and Cu-17%Cr-5%Al alloys with the objective of understanding the role of Al in influencing oxidation behavior. An examination of the phase diagrams shows that these are two phase alloys containing α-Cr and α-Cu [26,27,42,43]. In this regard, the key question to be answered is: Does Al addition to the Cu-17%Cr base alloy change the nature of the oxidation kinetics? The addition of 5% Al to the Cu-Cr composition was governed by earlier observations on MCrAl alloys that this is the minimum amount of Al required to form a protective alumina scale [41]. Thus, a second objective of this paper is to determine if the scale composition and microstructural characteristics are significantly altered by this amount of Al addition. There appears to be no previous research on the oxidation behavior of Cu-17%Cr-5%Al. The first part discusses the kinetics of the oxidation behavior of the two alloys while details of the scale compositions and microstructures are presented in the second part.

2. Experimental Procedures

The Cu-17%Cr and Cu-17%Cr-5%Al alloys were prepared by arc-melting chunks of high purity Al, Cr and Cu metals. These metals were carefully weighed in the appropriate amounts for the formulation of the correct composition and each charge was melted in an arc-melter under flowing argon. Care was taken in the melting procedures to ensure that each alloy preparation was re-melted and flipped several times in the arc melting furnace to homogenize the

composition of the melt before casting it into a button. Each button was then re-melted and drop cast into cylindrical copper molds to produce castings with the dimensions of the cylindrical region below the hot top approximately 13 mm diameter and 50 mm long. The alloys were homogenized annealed at 1223 K for 24 h under flowing argon to minimize elemental segregation. Figures 1(a) and (b) show the optical microstructures of the Cu-17%Cr and Cu-17%Cr-5%Al alloys, respectively, which essentially confirm that the alloys consist of two phases. Table 1 gives the composition of the two alloys, where the main elements were determined by the inductive coupled plasma (ICP) technique. Oxygen and nitrogen were determined by the inert gas fusion technique. In the case of the Cu-17%Cr-5%Al alloy, it was found necessary to conduct several measurements in order to minimize the effect of large segregated α-Cr particles on the results, where the weighted average from three measurements are reported in Table 1.

Oxidation disk specimens 12.7 mm in diameter and 2 mm thick were sliced from the cylindrical portions of each casting by wire electrodischarge machining (EDM). Although a number of specimens were sliced from the ingots, it was observed that many had shrinkage porosity thereby limiting the number of good specimens available for the oxidation tests. A 1.5 mm diameter hole was machined in each specimen about 1.5 mm from the edge to allow it to hang from Pt wires in the furnace during oxidation. The two faces of each specimen were polished to a final finish on 600 grit SiC paper to remove the EDM damaged layers and ultrasonically cleansed in ethanol prior to oxidation. Isothermal oxidation was conducted in a thermo-gravimetric analyzer (TGA) fitted with a Cahn-1000 microbalance, where the change in weight of the specimen was periodically recorded as a function of time by a computerized data

acquisition system. The oxidation tests were conducted between 773 and 1173 K for 100 h under dry flowing oxygen at 0.1 MPa, where the flow rate of the gas was 0.6 l/h (100 standard ccm). In the case of the Cu-17%Cr specimens, tests were conducted at absolute temperatures, T, between 773 and 973 K since there were insufficient good specimens to conduct tests at 1073 and 1173 K.

3. Results

3.1 Comparison of weight change data

Figures 2(a) & (b) compare the TGA specific weight change, $\delta W/A$, where δW is the change in weight of the specimen and A is the exposed area for oxidation[ii], as a function of time, t, for Cu-17% Cr and Cu-17%Cr -5%Al tested between 773 and 1173 K, respectively[iii]. The specific weight change is significantly larger for Cu-17%Cr compared to that for Cu-17%Cr-5%Al with the rate of oxidation decreasing with increasing time. In comparison, the Cu-17%Cr-5%Al alloy exhibits a very small or negligible weight change almost independent of time after a very short transient region in the temperature range 773-973 K. A longer transient region is observed at 1073 and 1173 K (Figs. 2(b)). The extent of the transient region is better depicted in Figs. 3(a-e), which show plots of the rate of specific weight change, $d(\delta W/A)/dt$, against t, for Cu-17%Cr and Cu-17%Cr-5%Al, respectively. An examination of Fig. 3 reveals that while the transient region for the Cu-17%Cr alloy lasts between 30 and 70 h, while that for the Cu-17%Cr-5%Al typically lasts less than 5 h for temperatures less than 1173 K; the transient region lasts for about 15 h at 1173 K. A distinct advantage of showing these rate change plots over the representation shown in Fig. 2 is that the steady-state oxidation regime can be clearly distinguished from the transient oxidation region thereby permitting an accurate and unbiased

[ii] This magnitude of A includes the sum of the areas of the two faces, the area of the outer edge of the specimen and the area of the specimen edge at the hole.
[iii] It is noted that t = 0 in this paper corresponds to the time at which the test temperature is attained.

determination of the rate constants for oxidation irrespective of the nature of the oxidation kinetics.

Figures 2 and 3 clearly demonstrate that a 5% Al addition to the Cu-17%Cr base composition significantly increases its oxidation resistance. Figure 4 also confirms this remarkable improvement in oxidation behavior, where the specific weight change data for the Cu-17%Cr-5%Al alloy determined at 1173 K is significantly lower than that for the Cu-17%Cr alloy measured at 773 K. Thus, the addition of this amount of Al results in at least a 400 K improvement in the temperature capabilities of the new alloy over Cu-17%Cr.

3.2 Oxidation rate equations

Although the parabolic rate equation is commonly used to describe the $\delta W/A - t$ relationships for many materials undergoing oxidation, it is well documented that other relationships can be important to describe the oxidation behavior of many alloys [10,15]. Assuming that the steady-state region of oxidation can be described by a generalized power-law relationship given by eqn. (1)

$$(\delta W/A)^m = k_m\, t \qquad (1)$$

where m is a constant and k_m[iv] is the appropriate oxidation rate constant, the magnitudes of k_m and m can be determined from double logarithmic plots of $\delta W/A$ and t without any *a priori* bias in the analysis [10]. Figures 5(a-e) show double logarithmic plots of $\delta W/A$ and t for Cu-17%Cr

[iv] In this paper, the subscripts 'm', 'p' and 'q' denote generic, parabolic and quartic relationships, respectively.

and Cu-17%Cr-5%Al between 773 and 1173 K. The figures also show linear regression lines fitted to the non-transient data.

Table 2 lists the values of k_m, m and the corresponding coefficients of determination, R_d^2, for the two alloys as a function of temperature describing these regression fits. The time range within which the data lie are also indicated. It is worth noting that the range of the steady-state oxidation regimes were defined to be consistent with Figs. 3(a-e) in this regression analyses so that care was taken to ensure that the $\delta W/A$ and t data pairs considered in the regression analyses were within this region. In the case of Cu-17%Cr-5%Al, the parabolic rate constants, k_p, were determined by linear regression analyses of the transient data within the first 15 h. The magnitudes of k_p for the oxidation of both Cu-17%Cr and Cu-17%Cr-5%Al were determined from $(\delta W/A)^2 - t$ data pairs (i.e. m = 2.0) by assuming that the intercepts are zero. On the other hand, the magnitudes of quartic rate constant, k_q, were determined by linearly regressing $\log(\delta W/A)$-log t data pairs lying in the time range shown in Table 2.

An examination of Figs. 5(a-e) and Table 2 reveals that the steady-state oxidation behavior of Cu-17%Cr is best described by a parabolic law, whereas the oxidation kinetics for the Cu-17%Cr-5%Al alloy is better represented by a quartic law. The regression equations fit the steady-state experimental data extremely well (Figs. 2(a-e)). Interestingly, the parabolic equations also represent the transient data fairly well in the case of the Cu-17%Cr-5%Al alloy. The parabolic oxidation kinetics observed for Cu-17%Cr in this investigation are consistent with similar observations for other Cu-Cr alloys [20,21]. Although no previous data appear to exist for the Cu-17%Cr-5%Al, the observation of quartic oxidation kinetics in the steady-state oxidation

regime in the temperature range 773-1173 K is self consistent. The transition from a parabolic relationship in the transient oxidation region to quartic rate kinetics in the steady-state oxidation regime between 973 and 1173 K suggests a change in the nature of the dominant oxidation mechanism presumably due to the effect of Al.

Using the constants given in Table 2, it is evident from Figs. 6(a-e) that the regressed equations fit the experimental data reasonably well for both alloys thereby confirming the general validity of these constants. In the case of Cu-17%Cr, the parabolic relationship with m = 2 does not describe the $\delta W/A$ data at 973 K as well as m = 1.6 especially in the transient regions of the plot. The quartic relationship describes the experimental observations on Cu-17%Cr-5%Al at 773 and 873 K throughout the entire time scale, and the latter portions of the curves between 973 and 1173 K, fairly well. However, the parabolic relationship better represents the initial set of data at the higher temperatures. Although it is unclear why the quartic relationship represents the data for Cu-17%Cr-5%Al better than the parabolic rate equation, it will be demonstrated later in Sec. 4.2 that the specific weight change data are better described by a logarithmic relationship.

3.3 Activation energies for oxidation

Figure 7 shows the variation of the rate constants, k_p and k_q, for Cu-17%Cr and Cu17%Cr-5%Al, respectively, as a function of the inverse of the absolute temperature in an Arrhenius plot. The activation energy for oxidation, Q, of Cu-17%Cr, as determined from the slope of the linear regression line through the datum points, is 165.9 ± 9.4 kJ mol^{-1} (R_d^2 = 0.997), where R_d^2 is the coefficient of determination and the errors represent the standard deviations about the regressed mean values, which is in excellent agreement with the value of

163 kJ mol^{-1} reported for Cu-29.5%Cr (35 vol.% Cr) [21]. These values are comparable to the value of 172 kJ mol^{-1} reported for the oxidation of high purity Cu oxidized in air or oxygen under 0.1 MPa pressure between 1073 and 1173 K, which was attributed to the outward lattice diffusion of Cu^{+} in Cu_2O [22]. It should be noted that the experimental activation energies for lattice diffusion of Cu^{+} and O^{--} in Cu_2O reported in the literature are about 150 and 165 kJ mol^{-1}, respectively, which were considered to be an insignificant difference by the authors [46].

In the case of Cu-17%Cr-5%Al, the experimental values of Q in the parabolic regime corresponding to the initial stages of oxidation were 24.9 ± 2.6 kJ mol^{-1} (R_d^2 = 0.989) between 773 and 973 K and increased to 117.6 ± 40.0 kJ mol^{-1} (R_d^2 = 0.896) above 973 K. For comparison, Tylecote [9] reported a value of 39 kJ mol^{-1} for oxidation of Cu between 573 and 773 K. The present observation of 24.9 kJ mol^{-1} is in excellent agreement with a value of 27 kJ mol^{-1} observed in the oxidation of 6N purity Cu in the temperature range 873 to 1023 K, and 38 kJ mol^{-1} in the oxidation of 2N purity Cu between 873 and 1223 K, corresponding to the oxidation of Cu_2O to CuO [47]. However, much higher values of Q = 186.5 ± 17.2 kJ mol^{-1} (R_d^2 = 0.975) independent of temperature were observed for the alloy in the steady-state quartic oxidation regime.

4. Discussion

4.1 Comparison with literature data

Figure 8 compares the temperature dependence of k_p determined for Cu-17%Cr and Cu-17%Cr-5%Al in the present investigation with those reported for Cu [6,9,10,16,18, 19,20,21,22,

44], Cu-Al [44, 45,48], Cu-Cr [20,21] and Cu-7(at.%)Cr-2%Al [44,45] alloys[v]. The typical magnitudes of k_p for alumina and chromia formers are also indicated for comparison [49]. It should be noted that Cu-10%Al was a two phase alloy since the it corresponds to the two phase region of the binary phase diagram [26,27].

An examination of Fig. 8 reveals two oxidation regimes for Cu. At temperatures exceeding 850 K, the temperature dependence of k_p is steeper than the trend in the data below this temperature. These two types of behavior have been attributed to oxidation mechanisms involving the lattice and grain boundary diffusion of Cu^+ in Cu_2O at high and low temperatures, respectively [22]. The addition of 1%Al appears to have no significant effect on the magnitudes of k_p but alloys containing 10%Al show a significant decrease in its value by about four orders of magnitude. In contrast, the addition of up to 50% Cr to Cu shows no significant decrease in the magnitude of k_p above the scatter in the data although the lattice diffusion controlled mechanism appears to be dominant even at 773 K. The data for Cu-75%Cr are too few and clustered to arrive at an unambiguous conclusion on whether this amount of Cr has had any effect on the magnitude of k_p. These observations demonstrate that Cr has no significant effect on the oxidation of as-cast Cu-Cr alloys.

The magnitudes of k_p determined for Cu-17%Cr in the present investigation are in reasonable agreement with the literature data. The k_p data for Cu-17%Cr-5%Al relating to the initial stages of oxidation are in agreement with the Cu-10%Al data within a factor of two. Three important points may be noted from these observations. First, the decrease in the k_p values is

[v] The parabolic rate constants show in Fig. 8 were determined from relatively short term tests lasting less than 24 h in most of the investigations. As shown in this investigation, oxidation to longer times can result in a change in the oxidation kinetics especially in Cu alloyed with Al.

almost entirely due to the addition of Al with no significant synergistic effect of Cr on the oxidation behavior of the alloy. Second, the transition temperature from grain boundary to lattice diffusion controlled oxidation appears to have increased from 850 K for pure Cu to 1073 K for both these Al containing alloys, although this observation is ambiguous due to the limited or clustered data. Third, the rate-controlling oxidation mechanisms are similar to those dominant in pure Cu during the early stage of oxidation but transitions to a different mechanism resulting in the observed quartic relationship during the later stages of oxidation. Clearly, Wagner's parabolic model is not applicable to the secondary stage of oxidation of Cu-17%Cr-5%Al.

Figure 9 compares the activation energies for oxidation of pure Cu [6,9,10,16,19,20, 21,22], Cu-Al [48], Cu-29.5%Cr [21] with those observed for Cu-17%Cr and Cu-17%Cr-5%Al in the present investigation[vi]. The activations energies for diffusion of Cu^{+} and O^{--} in Cu_2O, which were reported to be 150 and 165 kJ mol^{-1}, respectively [46], are indicated in the figure. It is now well established that the oxidation of Cu is controlled by the outward diffusion of Cu in the alloy to the metal-oxide interface and in the oxide scale [14,15,19,22]. An examination of Fig. 9 reveals that the experimental activation energies for Cu are clustered about three bands. Low values of $Q \approx 40$ kJ mol^{-1} have been attributed to the diffusion of Cu^{+} along the grain boundaries of Cu_2O [22]. However, it should be noted that theoretical calculations of the activation energy for copper vacancy migration in Cu_2O at room temperature predict a value of about 25 kJ mol^{-1} [50]. Intermediate values of $Q \approx 75$ to 125 kJ mol^{-1} have been attributed to either a mixture of grain boundary and lattice diffusion in Cu_2O [22] or diffusion of Cu^{+} in Cu_2O under conditions where only a single Cu_2O scale is stable [16,19]. Since CuO is stable only at

[vi] The terms "single" and "double" layers refer to the ideal scale morphologies consisting of either only a Cu_2O layer or a combination of an outer CuO layer over an inner Cu_2O layer, respectively.

high oxidation pressures, scale compositions at low partial pressures of oxygen consist predominantly of Cu_2O [10,19]. However, if oxidation occurs under conditions where CuO is stable, then the scale consists of an outer layer of CuO and an inner layer of Cu_2O leading to higher observed values of Q between 150 and 175 kJ mol^{-1}. These values compare fairly well with the reported values of activation energies for diffusion of Cu^+ and O^{--} in Cu_2O [46], although it has been suggested that the lattice diffusion of Cu^+ through the Cu_2O is the rate determining step for oxidation [22].

It is evident from Fig. 9 that the activation energy decreases from about 160 kJ mol^{-1} for Cu-1%Al to 90 kJ mol^{-1} for Cu-10%Al [48]. Correspondingly, the compositions of the scales formed on the Cu-1%Al and Cu-10%Al were CuO/Cu_2O and mostly Al_2O_3, respectively. The observed scale composition for Cu-1%Al is similar to that for pure Cu and consistent with the activation energies for oxidation observed in Cu for double scale formation (Fig. 10). However, the observation of mainly Al_2O_3 in the scale for Cu-10%Al for which $Q \approx 90$ kJ mol^{-1} is inconsistent with the typical values of $Q \approx 240$ kJ $mol^{-1}$for alumina forming Ni-based superalloys reported in the literature [51]. It is also noted that the activation energies for cation grain boundary and lattice diffusion in alumina are 477 and 419 kJ mol^{-1}, respectively, whereas those for anion grain boundary and lattice diffusion are 636 and 380 kJ mol^{-1}, respectively [52]. Interestingly, the addition of Cr to Cu has no significant effect on the magnitude of the activation energy, which is similar to those observed for double layer scale formation in Cu.

The activation energies for Cu-17%Cr-5%Al representative of the initial stages of oxidation increase from about 25 kJ mol^{-1} between 773 and 973 K to about 120 kJ mol^{-1} between

1073 and 1173 K (Fig. 9). Based on the observations on pure Cu, it would appear that the low value of 25 kJ mol^{-1} is due to grain boundary diffusion in Cu_2O at the lower temperatures and lattice diffusion in Cu_2O. It is reasonable to expect that the faster diffusion of Cu compared to Al and Cr would support the formation of an initial Cu_2O layer, which is consistent with the microstructural compositions of the oxide scale discussed in part II of this paper. The values of Q are independent of temperature and equal to about 185 kJ mol^{-1} in the quartic oxidation regime. It has been suggested that the activation energy for diffusion of Al in Cu is 165 kJ mol^{-1} [40]. However, since the activation energy for Cu-17%Cr was observed to be about 165 kJ mol^{-1}, it is ambiguous to attribute the observed value of $Q \approx 185$ kJ mol^{-1} to that due to Al diffusion in the alloy. It should be noted that the experimental value of Q lies between the lowest reported value of activation energy of 155 kJ mol^{-1} for the oxidation of pure Cu [10] and 240 kJ mol^{-1} for the oxidation of alumina forming alloys [51].

4.2 Effect of Al addition

Thus far, the analyses of the $(\delta W/A)$ - t data have assumed the validity of the power-law relationship given by eqn. (1). In the case of Cu-17%Cr, the parabolic relationship was shown to describe the data reasonably well over the entire time range between 773 and 973 K. In the case of Cu-17%Cr-5%Al the parabolic relationship is applicable for first 2 to 15 h depending on temperature after which a quartic relationship is obeyed. The addition of 5%Al to Cu-17%Cr resulted in a dramatic improvement in its oxidation properties (Fig. 4). An examination of Figs. 2-4 reveals that the specific weight gain for Cu-17%Cr was greater than that for Cu-17%Cr-5%Al by factors of 17 to 27 between 773 and 973 K after 100 h. A comparison of the parabolic oxidation constants for Cu-17%Cr and Cu-17%Cr-5%Al showed that the addition of 5%Al

resulted in a decrease in the magnitude of k_p by a factor of 2 to 4 in the temperature range 773 to 973 K. Since Cr had no significant effect on the oxidation of the binary as-cast Cu-Cr alloys, it must be concluded that this decrease in the magnitude of k_p is primarily due to the effect of Al.

Unlike the parabolic oxidation relationship, which has a physical basis in diffusion controlled mechanisms, such as Wagner's oxidation model [14,15], the quartic relationship observed in this study is strictly empirical at present based solely on an objective and consistent data analysis. Although quartic oxidation behavior has been reported in the literature for other alloys [14,15], there appears to be no physically based oxidation model at present to provide an insight into the causative nature of the oxidation process. Therefore, it is instructive to examine the degree of statistical fit of other equations reported in the literature to the present ($\delta W/A$) – t data for Cu-17%Cr-5%Al.

Alternative to the power-law relation eqn. (1), it is worthwhile to examine whether a logarithmic relationship would describe the ($\delta W/A$) - t data as well, especially since as discussed in part II of the paper, the oxide scales formed on the Cu-17%Cr-5%Al specimens were very thin. The ($\delta W/A$)-t data were regressed with the following logarithmic relationship to determine the regression parameters [14]:

$$(\delta W/A) = k_{log} \log (t+1) + A \qquad (2)$$

where k_{log} and A are fitting constants. Figure 10 demonstrates that the variation of the experimentally measured values of ($\delta W/A$) with log (t+1) is approximately linear and Table 3

gives the regressed magnitudes of k_{log}, A and R_d^2. It is evident that equation (2) describes the experimental data fairly well. In fact, a comparison of the regression fits to the experimental data for the logarithmic and quartic equations revealed an excellent correlation with the entire time span of the data for the former relationship at all temperatures (Fig. 11). The magnitudes of the activation energies determined from a semi-logarithmic plot of k_{log} against 1/T resulted in Q ≈ 33 kJ mol^{-1} between 773 and 1073 K and 115 kJ mol^{-1} between 1073 and 1173 K (Fig. 12). These values are similar to those determined from the parabolic rate constants.

The observed excellent correlation between eqn. (2) and the experimental specific weight change data (Fig. 10) is encouraging because a number of models have been proposed to describe low temperature oxidation, where the time dependent change in the thickness of a thin scale usually follows a logarithmic relationship [14,15]. An important point to note is that generally logarithmic rate equations describing the growth of thin scales are best suited for low temperature conditions, where the rates of diffusion of the reacting species are relatively small. In the present study, the test temperatures were sufficiently high to ensure higher rates of diffusion of the reacting species. This is certainly the case for the Cu-17%Cr alloy reported in this paper as well as for other Cu-Cr alloys [20,21], where the parabolic rate law and the observance of thick Cu_2O and CuO scales formed a consistent picture. The fact that the addition of 5%Al to the base composition dramatically increased its oxidation resistance can be attributed to one or more factors, such as the formation of a protective oxide scale and a slower rate of diffusion of Cu^+ in Cu_2O due to a change in its defect chemistry. In this connection, it is interesting to note that theoretical calculations suggest that the presence of Al in Cu_2O binds it to copper vacancies, V_{Cu}, with a binding energy of about 320 kJ mol^{-1} thereby inhibiting V_{Cu}

diffusion in Cu_2O with the activation energy for the diffusion of V_{Cu} in Cu_2O calculated to be about 25 kJ mol^{-1} [50]. This theoretical value of 25 kJ mol^{-1} is in excellent agreement with the value of $Q \approx 33$ kJ mol^{-1} determined in the present study using the logarithmic equation (Fig. 12). Therefore, it appears reasonable to suggest that the inhibition of Cu^+ diffusion in Cu_2O by Al is the predominant mechanism governing oxidation behavior of the Cu-17%Cr-5%Al below 1073 K and the growth of a protective alumina scale above 1073 K is the dominant process.

Summary and Conclusions

The effect of 5% Al on the oxidation behavior of Cu-17%Cr was investigated. It was demonstrated that adding 5% Al resulted in:

a) A decrease in the parabolic oxidation rate by factors of 100 to 1000 compared to pure Cu and Cu-17%Cr.
b) An increased temperature capability up to 400 K compared to Cu-17%Cr.
c) A change from parabolic oxidation kinetics for Cu-17% Cr to either a quartic or logarithmic rate law for Cu-17%Cr-5%Al.

The parabolic rate constants determined for Cu-17%Cr between 773 and 973 K were similar to those reported for pure Cu [6,9,10,16,18,19,20,21,22,44], Cu-1%Al [44,45,48] and Cu-Cr [20,21] alloys, while the activation energy for oxidation of the alloy was 165 kJ mol^{-1}. This value of activation energy was comparable to the diffusion of Cu^+ ions in pure Cu [22] and Cu-Cr alloys [21] oxidized under relatively high partial pressures of oxygen to form CuO/Cu_2O scales. It was concluded that Cr did not improve the oxidation behavior of as-cast Cu-17%Cr.

The oxidation kinetics for Cu-17%Cr-5%Al were more complex than pure Cu and Cu-17%Cr in the temperature range 773-1173 K. The initial variations in the specific weight change data with time were better described by a parabolic relationship while the latter portions of the specific weight change curves were better described by a quartic function. Using the parabolic relationship corresponding to the initial oxidation regime, the values of Q were observed to vary from 25 kJ mol^{-1} between 773 and 973 K an increased to 115 kJ mol^{-1} above 973 K. However, using the quartic relationship corresponding to the steady-state oxidation region, the value of Q was observed to be 185 kJ mol^{-1}. The weight change data could be better described by a logarithmic relationship, where the activation energy for oxidation increased from about 35 kJ mol^{-1} between 773 and 1073 K to 115 kJ mol^{-1} above 1073 K. Comparisons of the parabolic rate constants with literature data on Cu [6,9,10,16,18,19,20,21,22,44], Cu-Al [44,48], Cu-Cr [20,21], Cu-7%Cr-2%Al [44,45], and alumina [49] and chromia [49] scale formers revealed that the k_p values for Cu-17%Cr-5%Al were significantly less than those for Cu, Cu-1%Al and Cu-Cr alloys by factors of 100 to 1000. These values were also less than those published for chromia scale forming alloys published in the literature [49] but close to those reported for alumina scale formers [49] and Cu-10%Al [48] and Cu-7(at.%)Cr-2%Al [44,45] alloys. The activations energies determined using either the parabolic rate constants or the logarithmic rate constants were similar and varied from about 25-35 kJ mol^{-1} below 1073 K to 115 kJ mol^{-1} at higher temperatures. The values of activation energy at the lower temperatures are in excellent agreement with the theoretical value of 25 kJ mol^{-1} calculated for the diffusion of V_{Cu} diffusion in Al doped Cu_2O, where the Al atoms are predicted to bind to the copper vacancies [50]. Therefore, it is suggested that the inhibition of Cu^+ diffusion in Cu_2O by Al is the predominant

mechanism governing oxidation behavior of the Cu-17%Cr-5%Al below 1073 K. It is expected that the growth of a protective alumina scale will be the dominant process above 1073 K.

Acknowledgements

The author thanks Mr. Donald Humphrey for conducting the isothermal oxidation tests and Mr. Dereck Johnson for conducting chemical analyses of the specimens.

References

1. H. J. Kasper, in: S. F. Morea and S. T. Wu (Eds.), *Advanced High Pressure O_2/H_2 Technology*, NASA CP 2372 (George C. Marshall Space Flight Center, Huntsville, AL, 1985), pp. 36-43.
2. D. B. Morgan, A. C. Kobayashi, *Main Combustion Chamber and Cooling Technology Study – Final Report*, NASA CR 184345 (NASA Marshall Space Flight Center, Huntsville, AL, 1989).
3. L. Ogbuji and D. L. Humphrey, Oxid. Metals **60**, 271-291 (2003).
4. E. Scheil, Zeit. für Metallkde. **29**, 209-214 (1937); translated version in NACA-TM-1338, National Advisory Committee for Aeronautics, Washington, D.C. (1952).
5. H. Nishimura, J. Suiyokwaishi **9**, 655-664 (1938).
6. G. Valensi, *Pittsburgh International Conference on Surface Reactions*, Electrochemical Society, Pittsburgh, PA (1948).
7. R. F. Tylecote, J. Inst. Metals **78**, 259-300 (1950-51).
8. R. F. Tylecote, J. Inst. Metals **78**, 301-326 (1950-51).
9. R. F. Tylecote, J. Inst. Metals **78**, 327-350 (1950-51).
10. D. W. Bridges, J. P. Baur, G. S. Baur and W. M. Fassell, J. Electrochem. Soc. **103**, 475-478 (1956).
11. P. Kofstad, Nature **179**, 1362-1363 (1957).
12. J. A. Sartell and C. H. Li, Trans. ASM **55,** 58-162 (1962).
13. L. Czerski, S. Mrowec and T. Weber, Roczniki Chem. **38**, 643-654 (1964).
14. P. Kofstad, *High-Temperature Oxidation of Metals* (John Wiley, New York, NY, 1966).
15. O. Kubaschewski and B. E. Hopkins, *Oxidation of Metals and Alloys* (Butterworths, London, U.K., 1967).
16. S. Mrowec and A. Stoklosa, Oxid. Metals **3**, 291-311 (1971).
17. P. C. Donovan and C. J. Barton, Metall. Trans. **4**, 1765-1767 (1973).

18. F. Gesmundo, C. De Asmundis and S. Merlo, Werkstofe Und Korrosion - Materials and Corrosion vol 30, 114 (1979).

19. J. H. Park and K. Natesan, Oxid. Metals **39**, 411-435 (1993).

20. Y. Niu, F. Gesmundo, F. Viani and D. L. Douglass, Oxid. Metals **48**, 357-380 (1997).

21. K. T. Chiang, G. H. Meier and F. S. Pettit in: S. B. Newcombe and J. A. Little (Eds.), *Microscopy of Oxidation* (The Institute of Metals, London, U.K., 1997).

22. Y.Zhu, K. Mimura, J W. Lim, M. Isshiki and Q. Jiang, Metall. Mater. Trans. A **37A**, 1231-1237 (2006).

23. F. Gesmundo, Y. Niu, F. Viani and D. L. Douglass, Oxid. Metals **49**, 147-167 (1998).

24. G. Y. Fu, Y. Niu and F. Gesmundo, Corr. Sci. **45**, 559-574 (2003).

25. L. U. Ogbuji, Surf. Coat. Tech. **197**, 327-335 (2005).

26. D. J. Chakrabarti and D. E. Laughlin, Bull. Alloy Phase Diagrams **5**, 59 (1984).

27. T. B. Massalski, H. Okamoto and P. R. Subramanian (Eds.), *Binary Alloy Phase Diagrams* (ASM International, Materials Park, Cleveland, OH 1990).

28. K. T. Chiang, P. D. Krotz and J. L. Yuen, Surf. Coat. Technol. **76**, 14-19 (1995).

29. K. T. Chiang and J. P. Ampaya, Surf. Coat. Technol. **78**, 243-247 (1996).

30. T. A. Wallace, R. K Clark and K. T. Chiang, J. Spacecraft Rockets **35**, 546-51 (1998).

31. S. V. Raj, L. J. Ghosn, C. Robinson and D. Humphrey, Mater. Sci. Eng. A **457**, pp. 300-312 (2007).

32. S. V. Raj, unpublished research, NASA Glenn Research Center, Cleveland, OH (2003).

33. J. S. Dunn, J. Inst. Metals **46**, 25- (1934).

34. K. W. Frohlich, Zeits. Metallkunde. **28**, 368- (1936).

35. L. E. Price and G. J. Thomas, J. Inst. Metals **63**, 21- (1938).

36. J. P. Dennison and A. Preece, J. Inst. Metals **81**, 229-234 (1952).

37. J. C. Blade and A. Preece, J. Inst. Metals **88**, 427-432 (1959).

38. M. D. Saderson and J. C. Scully, Oxid. Metals **3**, 59-90 (1971).

39. K. Hauffe and E. Ofulue, Werkst. Korros. – Mater. Corr. **23**, 351-355 (1972).

40. G. Plascencia, T. Utigard and T. Marín, JOM **57**, 80-84 (2005).

41. J. L. Smialek and G. H. Meier in: C. T. Sims, N. S. Stoloff and W. C. Hagel (Eds.), *Superalloys II* (John Wiley, New York, 1987) pp. 293-326.

42. G. Ghosh in: G. Petzow and G. Effenberg (Eds.), *Handbook of Ternary Alloy Phase Diagrams,* **vol. 4** (VCH Publishers, New York, NY, 1991), pp. 311-319.

43. B. Grushko, E. Kowalska-Strzeciwilk, B. Przepiorzynski and M. Surowiec, J. Alloys and Compounds **417**, 121-126 (2006).

44. Y. Niu, S. Y. Wang and F. Gesmundo, Oxid. Metals **65**, 285-306 (2006).

45. S. Y. Wang, F. Gesmundo, W. T. Wu and Y. Niu, Scripta Mater. **54**, 1563-1568 (2006).

46. W. J. Moore, Y. Ebisuzaki and J. A. Sluss, J. Phys. Chem. **62**, 1438-1441 (1958).

47. Y. Zhu, K. Mimura and M. Isshiki, Oxid. Metals **62**, 207-222 (2004).

48. W. Kai, G. W. Fan, P. C. Chen and Y. T. Lin, Oxid. Metals **61**, 439-461 (2004).

49. H. Hindam and D. P. Whittle, Oxid. Metals **18**, 245-284 (1982).

50. A. F. Wright and J. S. Nelson, J. Appl. Phys. **92**, 5849-5851 (2002).

51. R. H. Doremus, J. Appl. Phys. **95**, 3217-3222 (2004).

52. H. J. Frost and M. F. Ashby, *Deformation-Mechanism Maps: The Plasticity and Creep of Metals and Ceramics* (Pergamon Press, Oxford, 1982) p. 99.

Table 1: Compositions of the as-cast and heat treated alloys with nominal compositions of Cu-17%Cr and Cu-17%Cr-5%Al in wt.%.

Nominal composition	Al	Cr	Cu	Fe	N	O	Remarks
Cu-17%Cr	0.05	15.6	84.2	0.0050	0.0003	0.0700	Readings from one specimen
Cu-17%Cr-5%Al	4.78	17.8	77.4	0.0013	0.0002	0.0048	Weighted average of three large pieces (> 400 mg)

Table 2: Magnitudes of the oxidation rate constants for Cu-17%Cr and Cu-17%Cr-5%Al alloys between 773 and 1173 K determined from the steady-state oxidation region of the log(δW/A) vs. log t plots (Fig. 5).

	773 K			873 K			973 K			1073 K			1173 K		
	m	**k_m**	**R_d^2**	**m**	**k_m**	**R_d^2**	**m**	**k_m**	**R_d^2**	**m**	**k_m**	**R_d^2**	**m**	**k_m**	**R_d^2**
Cu-17Cr ($mg^2/mm^4/s$) (parabolic) (time range analyzed)	2.0	$1.7x10^{-9}$ (39-100 h)	0.999	2.0	$2.6x10^{-8}$ (49.6-100 h)	0.998	2.0	$3.5x10^{-7}$ (60-100 h)	0.992	-	-	-	-	-	-
Cu-17Cr-5Al ($mg^2/mm^4/s$) (parabolic) (time range analyzed)	2.0	$1.6x10^{-11}$ (0-1.9 h)	0.981	2.0	$2.4x10^{-11}$ (0-11 h)	0.982	2.0	$3.7x10^{-11}$ (0-15 h)	0.987	2.0	$7.0x10^{-11}$ (0-15 h)	0.987	2.0	$4.6x10^{-10}$ (0-15 h)	0.999
Cu-17Cr-5Al ($mg^4/mm^8/s$) (quartic) (time range analyzed)	4.3	$2.4x10^{-19}$ (2.2-100 h)	0.885	4.3	$2.4x10^{-18}$ (15-100 h)	0.810	4.4	$5.6x10^{-17}$ (19.6-100 h)	0.983	3.7	$1.4x10^{-15}$ (22-100 h)	0.994	4.4	$2.2x10^{-15}$ (30-100 h)	0.972

Note: Units for k_m are $(mg/mm^2)^m$.

Table 3: Regression coefficients for Cu-17%Cr-5%Al using the direct logarithmic rate equation, $(\delta W/A) = k_{log} \log(t+1) + A$.

773 K			873 K			973 K			1073 K			1173 K		
k_{log}	**A**	**R_d^2**	**k_{log}**	**A**	**R_d^2**	**k_{log}**	**A**	**R_d^2**	**k_{log}**	**A**	**R_d^2**	**k_{log}**	**A**	**R_d^2**
3.8×10^{-4}	1.3×10^{-4}	0.890	6.9×10^{-4}	1.5×10^{-4}	0.926	1.1×10^{-3}	7.6×10^{-5}	0.997	1.5×10^{-3}	6.8×10^{-5}	0.996	4.5×10^{-3}	-4.1×10^{-4}	0.995

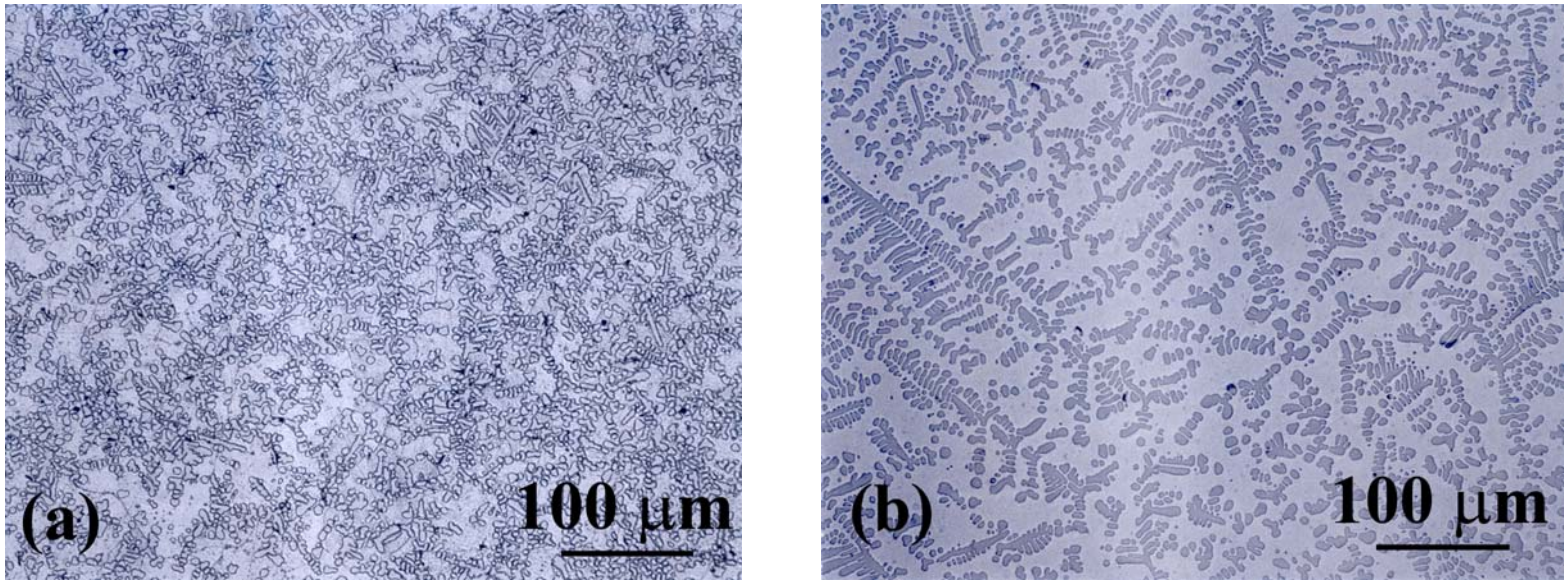

Fig. 1 Optical microstructures of as-cast (a) Cu-17%Cr and (b) Cu-17%Cr-5%Al alloys.

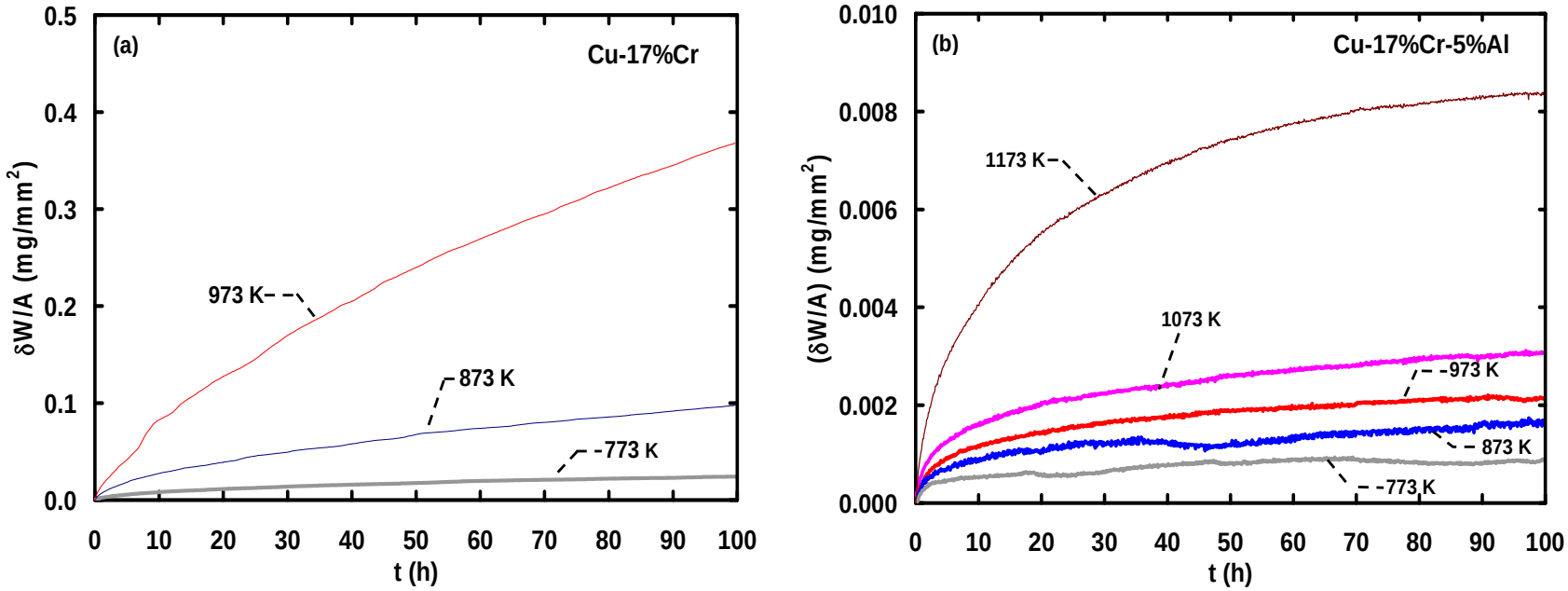

Fig. 2 Specific weight change vs. time plots for (a) Cu-17%Cr and (b) Cu-17%Cr-5%Al between 773 and 1173 K.

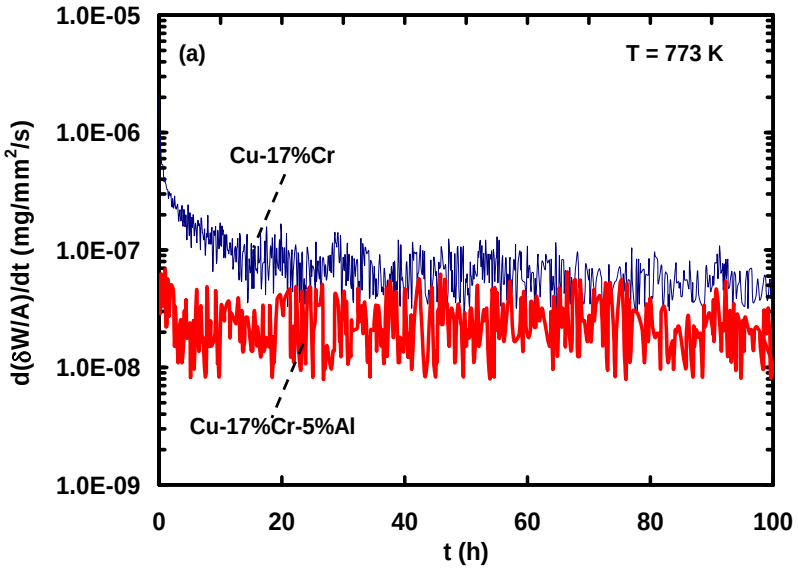
(a)
T = 773 K
Cu-17%Cr
Cu-17%Cr-5%Al
d(δW/A)/dt (mg/mm²/s)
t (h)
1.0E-05
1.0E-06
1.0E-07
1.0E-08
1.0E-09
0
20
40
60
80
100

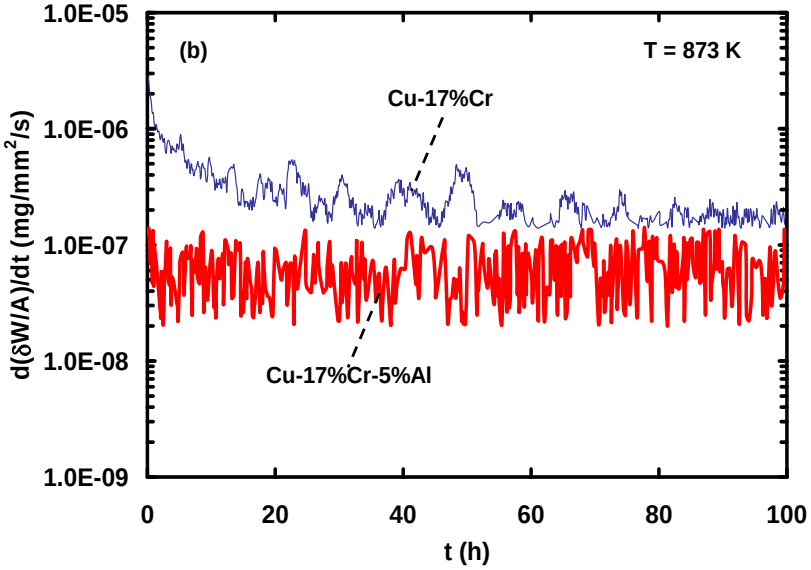
(b)
T = 873 K
Cu-17%Cr
Cu-17%Cr-5%Al
d(δW/A)/dt (mg/mm²/s)
t (h)
1.0E-05
1.0E-06
1.0E-07
1.0E-08
1.0E-09
0
20
40
60
80
100

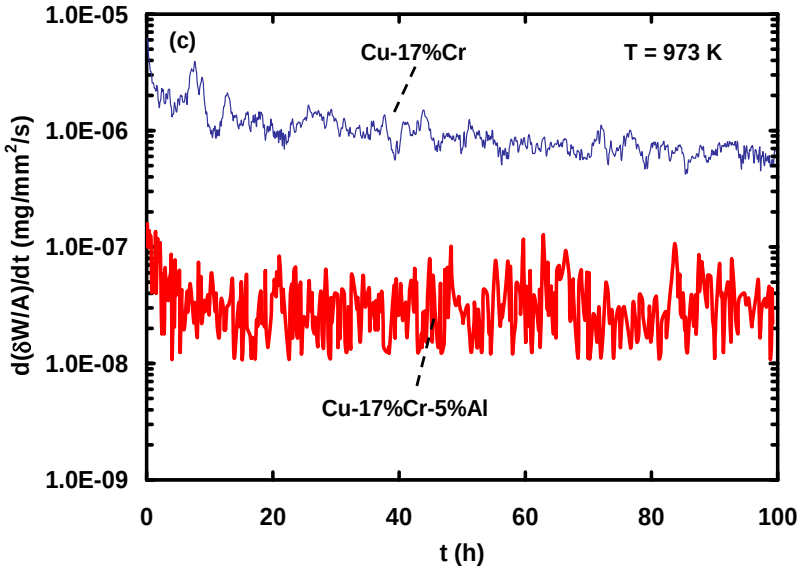
(c)
T = 973 K
Cu-17%Cr
Cu-17%Cr-5%Al
d(δW/A)/dt (mg/mm²/s)
t (h)
1.0E-05
1.0E-06
1.0E-07
1.0E-08
1.0E-09
0
20
40
60
80
100

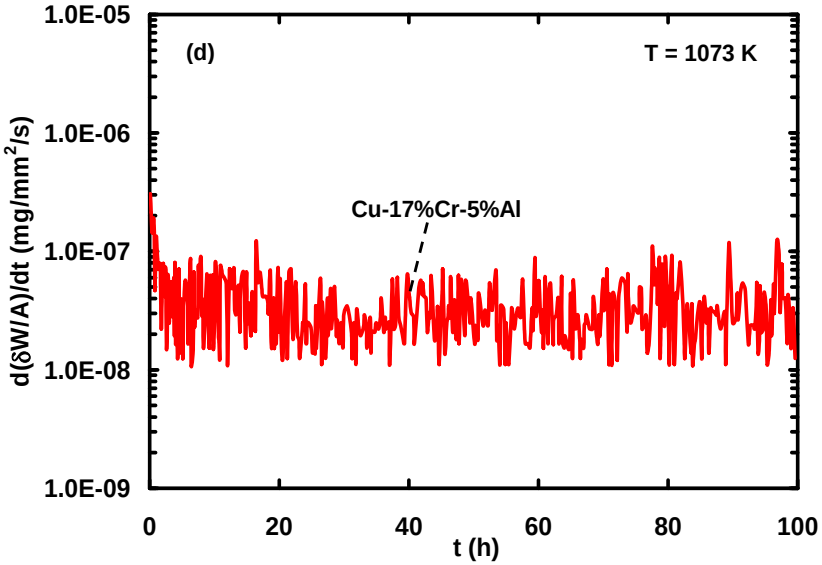
(d)
T = 1073 K
Cu-17%Cr-5%Al
d(δW/A)/dt (mg/mm²/s)
t (h)
1.0E-05
1.0E-06
1.0E-07
1.0E-08
1.0E-09
0
20
40
60
80
100

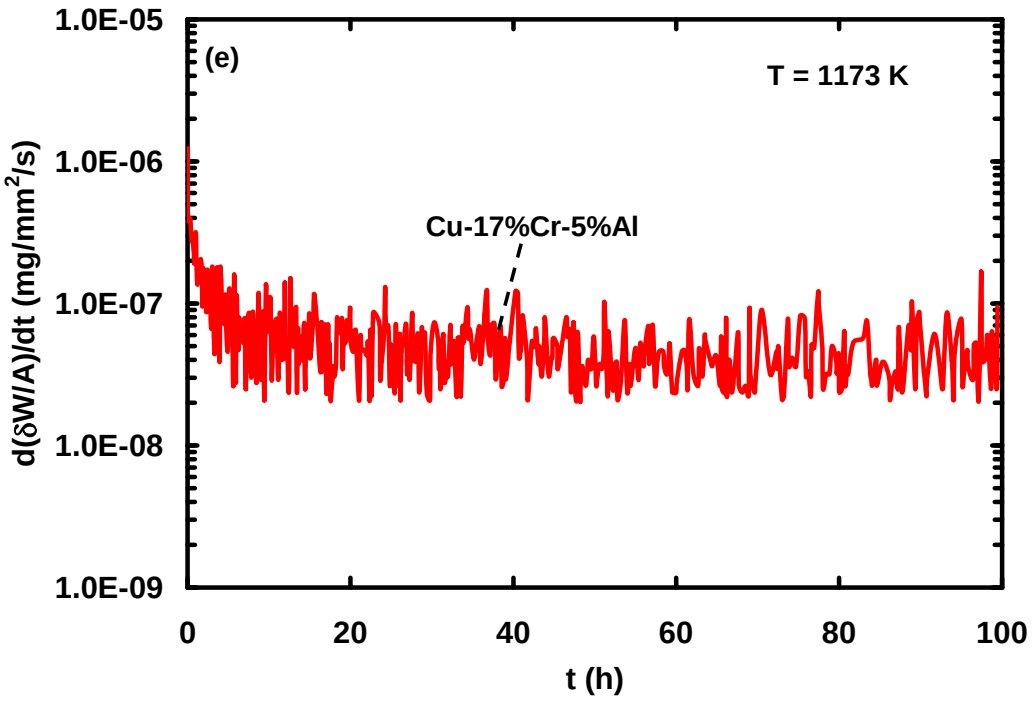

Fig. 3 Variation of the rate of the specific weight change with time for Cu-17%Cr and Cu-17%Cr-5%Al; (a) 773 K; (b) 873 K; (c) 973 K; (d) 1073 K; (e) 1173 K.

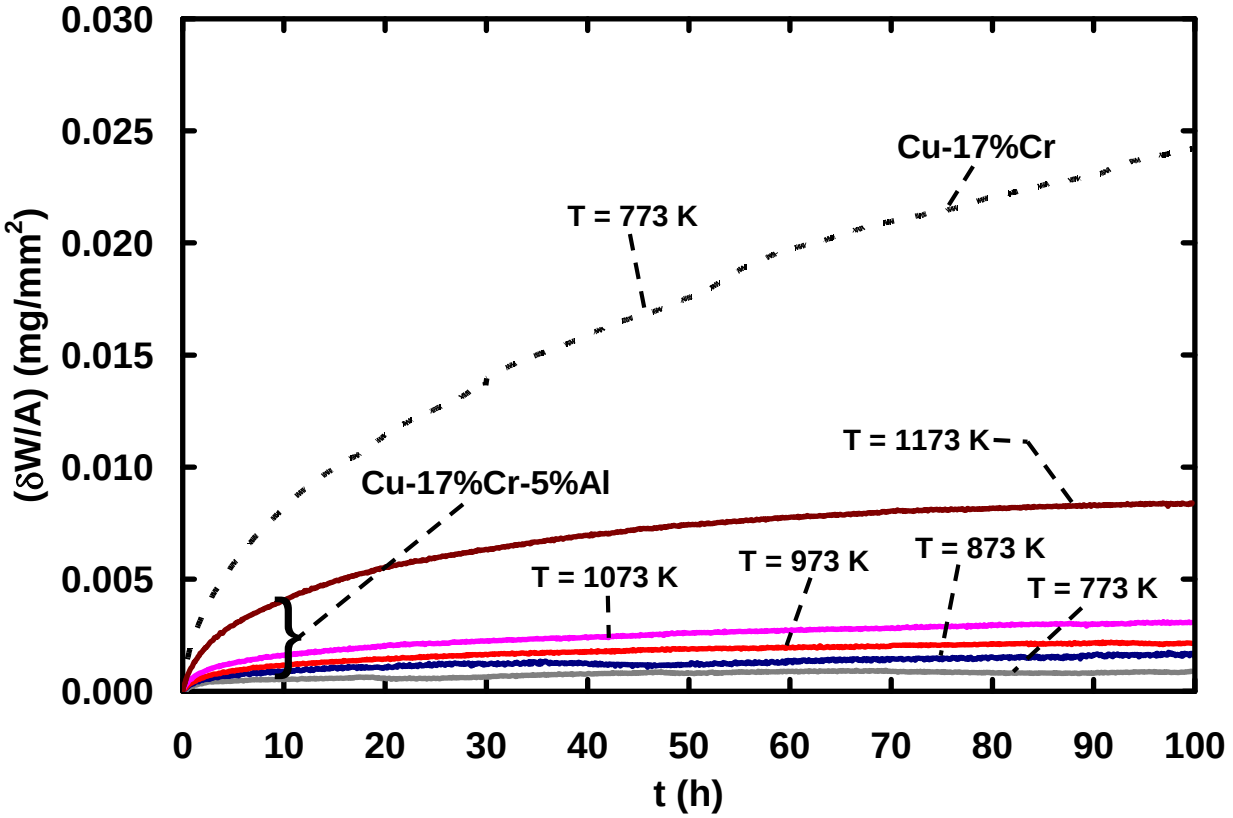

Fig. 4 Comparison of the specific weight change data for Cu-17%Cr determined at 773 K with those for Cu-17%Cr-5%Al determined between 773 and 1173 K demonstrating the superior oxidation behavior of the Al containing alloy.

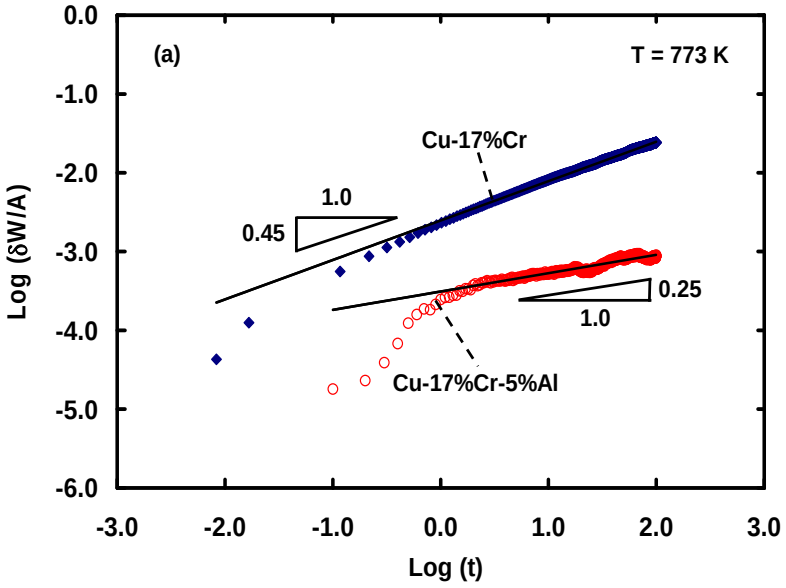
(a)
T = 773 K
Cu-17%Cr
1.0
0.45
0.25
1.0
Cu-17%Cr-5%Al
Log (δW/A)
Log (t)
0.0
-1.0
-2.0
-3.0
-4.0
-5.0
-6.0
-3.0
-2.0
-1.0
0.0
1.0
2.0
3.0

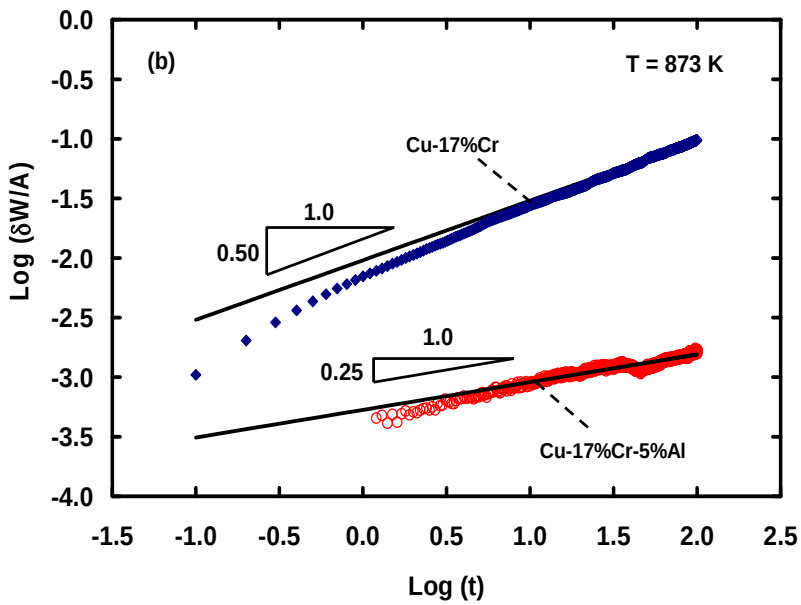
(b)
T = 873 K
Cu-17%Cr
1.0
0.50
1.0
0.25
Cu-17%Cr-5%Al
Log (δW/A)
Log (t)
0.0
-0.5
-1.0
-1.5
-2.0
-2.5
-3.0
-3.5
-4.0
-1.5
-1.0
-0.5
0.0
0.5
1.0
1.5
2.0
2.5

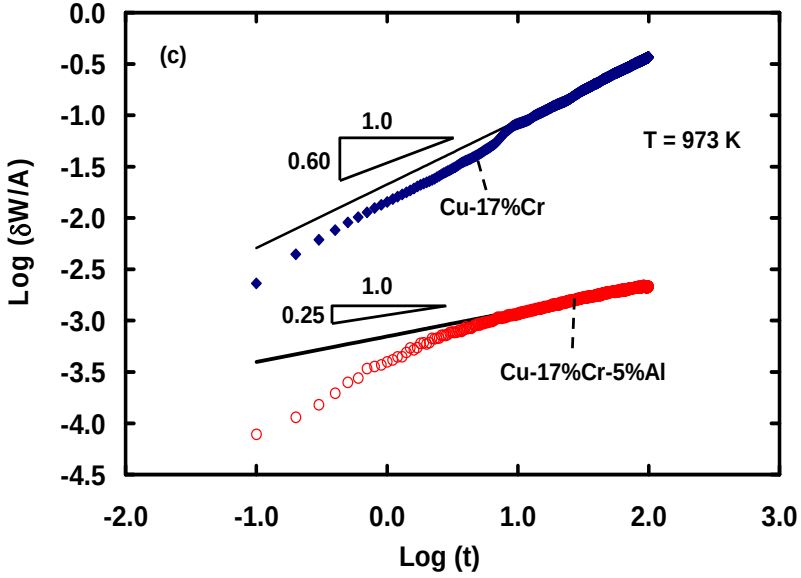
(c)
T = 973 K
1.0
0.60
Cu-17%Cr
1.0
0.25
Cu-17%Cr-5%Al
Log (δW/A)
Log (t)
0.0
-0.5
-1.0
-1.5
-2.0
-2.5
-3.0
-3.5
-4.0
-4.5
-2.0
-1.0
0.0
1.0
2.0
3.0

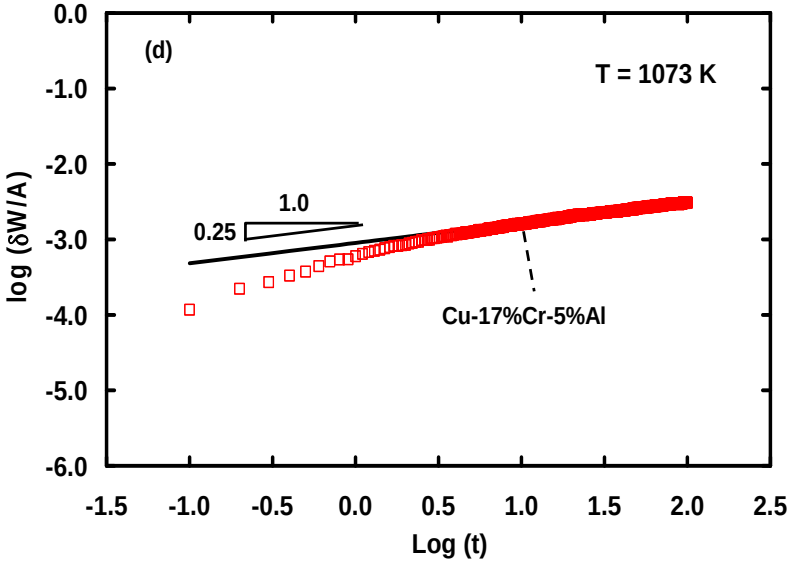
(d)
T = 1073 K
1.0
0.25
Cu-17%Cr-5%Al
log (δW/A)
Log (t)
0.0
-1.0
-2.0
-3.0
-4.0
-5.0
-6.0
-1.5
-1.0
-0.5
0.0
0.5
1.0
1.5
2.0
2.5

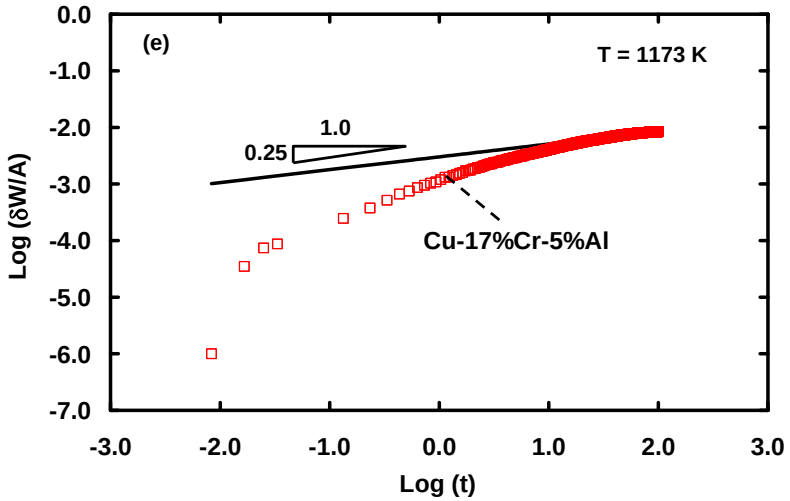

Fig. 5 Double logarithmic plots showing the variation of the specific weight change with time for Cu-17%Cr and Cu-17%Cr-5%Al; (a) 773 K; (b) 873 K; (c) 973 K; (d) 1073 K; (e) 1173 K.

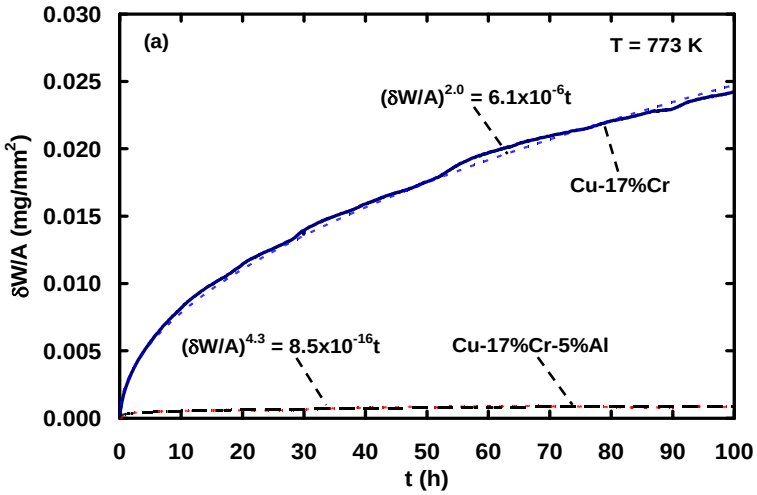
(a)
T = 773 K
$(\delta W/A)^{2.0} = 6.1x10^{-6}t$
Cu-17%Cr
$(\delta W/A)^{4.3} = 8.5x10^{-16}t$
Cu-17%Cr-5%Al
δW/A (mg/mm²)
t (h)

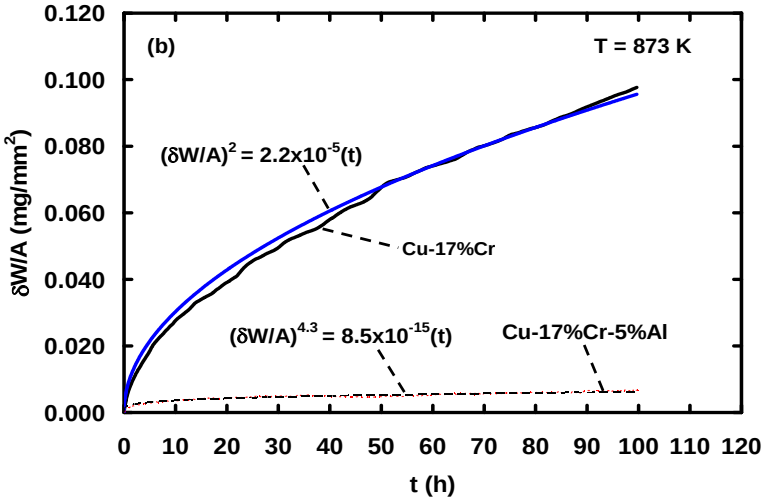
(b)
T = 873 K
$(\delta W/A)^{2} = 2.2x10^{-5}(t)$
Cu-17%Cr
$(\delta W/A)^{4.3} = 8.5x10^{-15}(t)$
Cu-17%Cr-5%Al
δW/A (mg/mm²)
t (h)

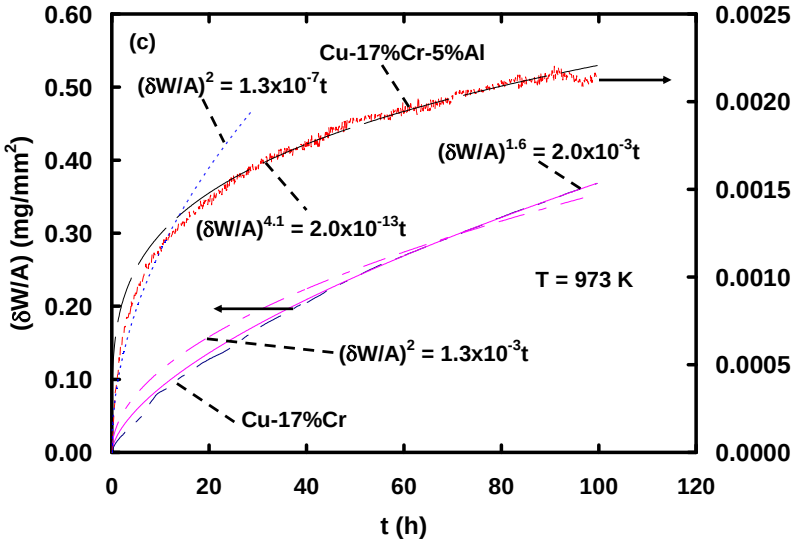
(c)
Cu-17%Cr-5%Al
$(\delta W/A)^{2} = 1.3x10^{-7}t$
$(\delta W/A)^{1.6} = 2.0x10^{-3}t$
$(\delta W/A)^{4.1} = 2.0x10^{-13}t$
T = 973 K
$(\delta W/A)^{2} = 1.3x10^{-3}t$
Cu-17%Cr
(δW/A) (mg/mm²)
t (h)

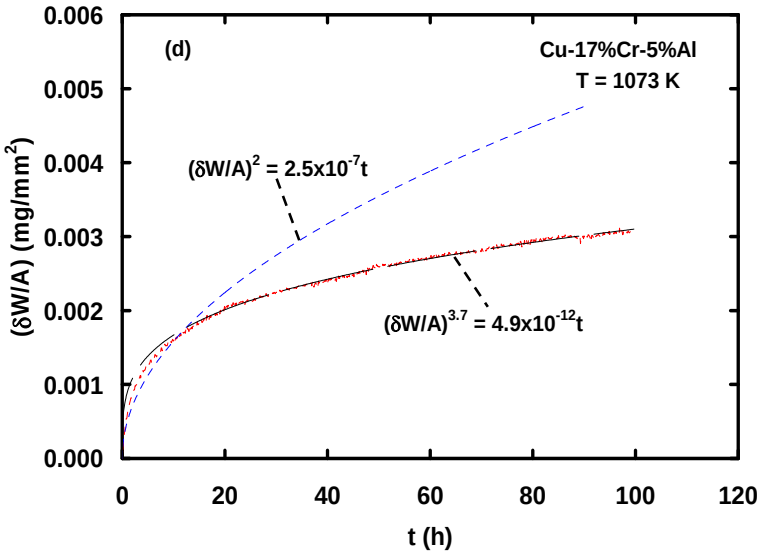
(d)
Cu-17%Cr-5%Al
T = 1073 K
$(\delta W/A)^{2} = 2.5x10^{-7}t$
$(\delta W/A)^{3.7} = 4.9x10^{-12}t$
(δW/A) (mg/mm²)
t (h)

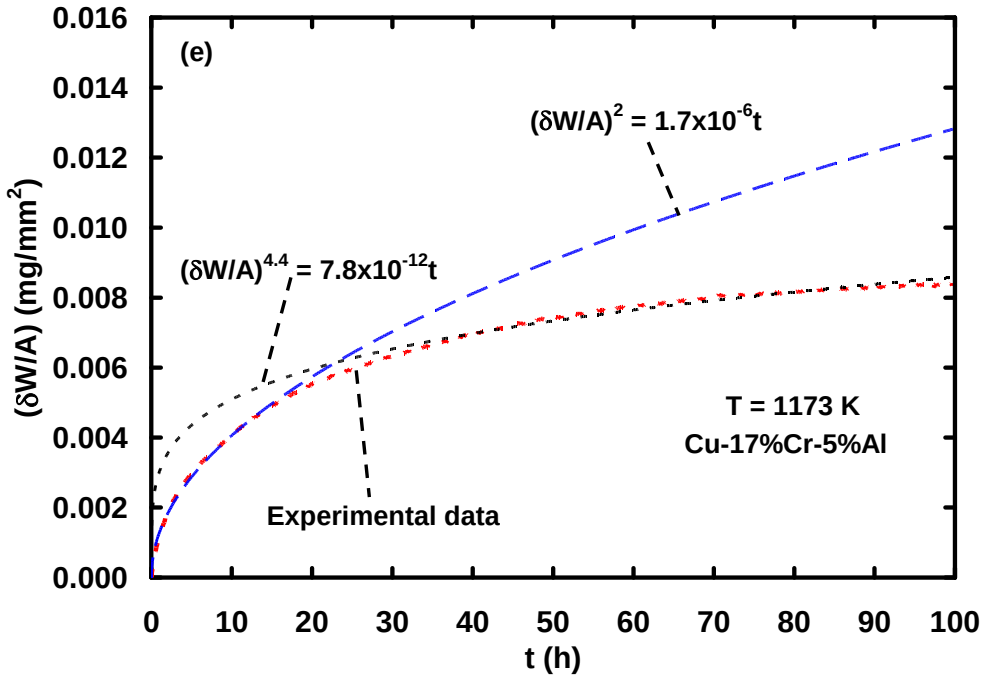

Fig. 6 Comparison of the regression equations with experimental data for Cu-17%Cr and Cu-17%Cr-5%Al; (a) 773 K; (b) 873 K; (c) 973 K; (d) 1073 K; (e) 1173 K.

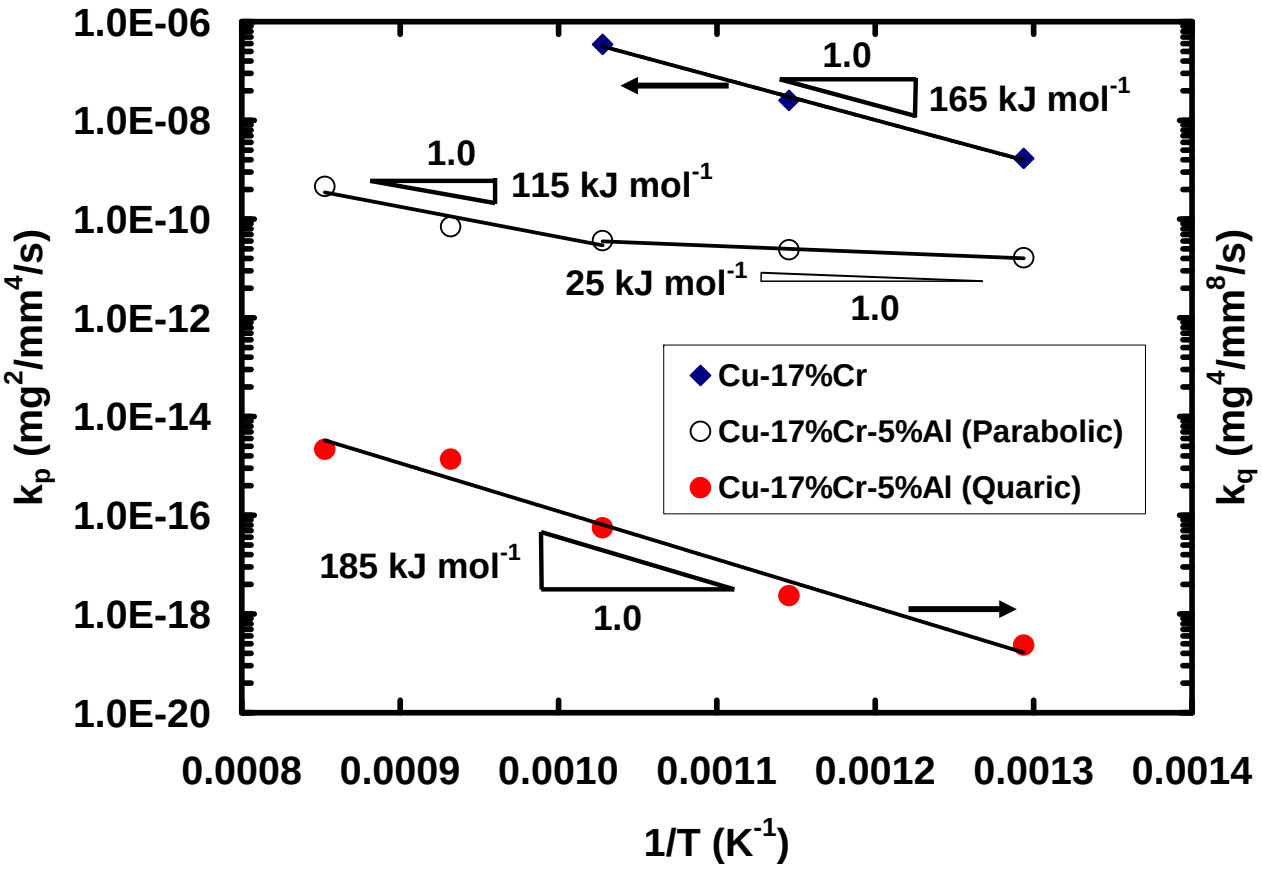

Fig. 7 Arrhenius plot showing the temperature dependence of the parabolic and quartic rate constants for Cu-17%Cr and Cu-17%Cr-5%Al.

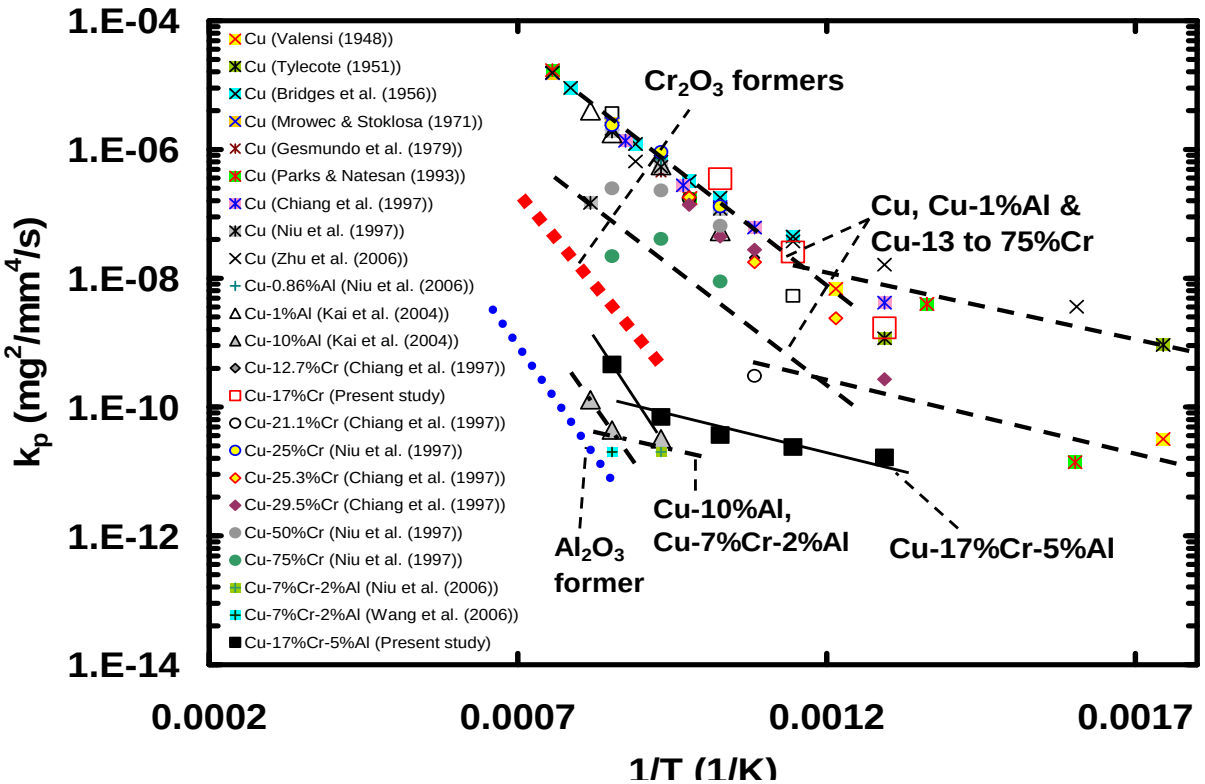

Fig. 8 Arrhenius plot comparing the parabolic rate constants for Cu [6,9,10,16,18,19,20,21,22,44], Cu-Al [44,45,48], Cu-Cr [20,21] and Cu-7(at.%)Cr-2%Al [44, 45,] reported in the literature with data obtained on Cu-17%Cr and Cu-17%Cr-5%Al in the present study.

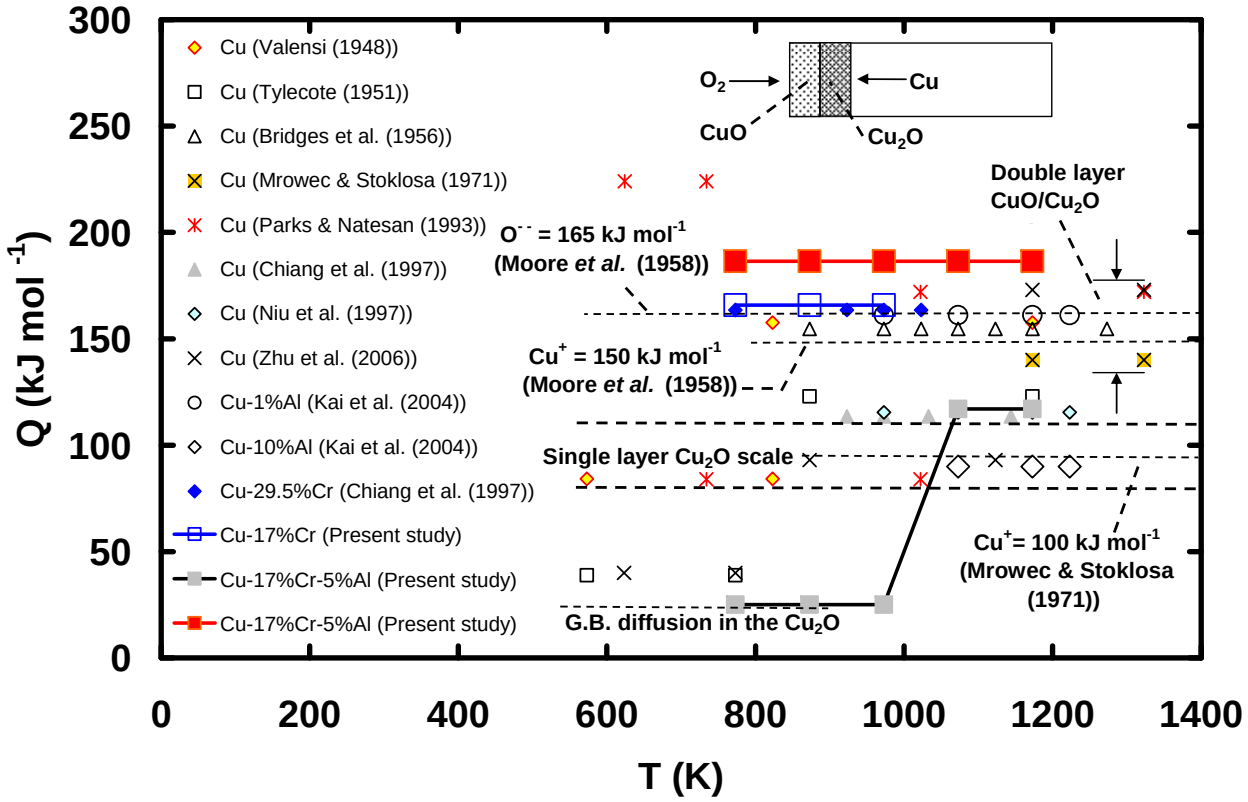

Fig. 9 Comparison of the activation energies for oxidation of pure Cu [6,9,10,16,19,20,21,22], Cu-Al [48], Cu-29.5%Cr [21] with those for Cu-17%Cr and Cu-17%Cr-5%Al. The lower values of activation energies for oxidation of Cu-17%Cr-5%Al were determined using the parabolic relationship, whereas the higher values were determined from the quartic relationship.

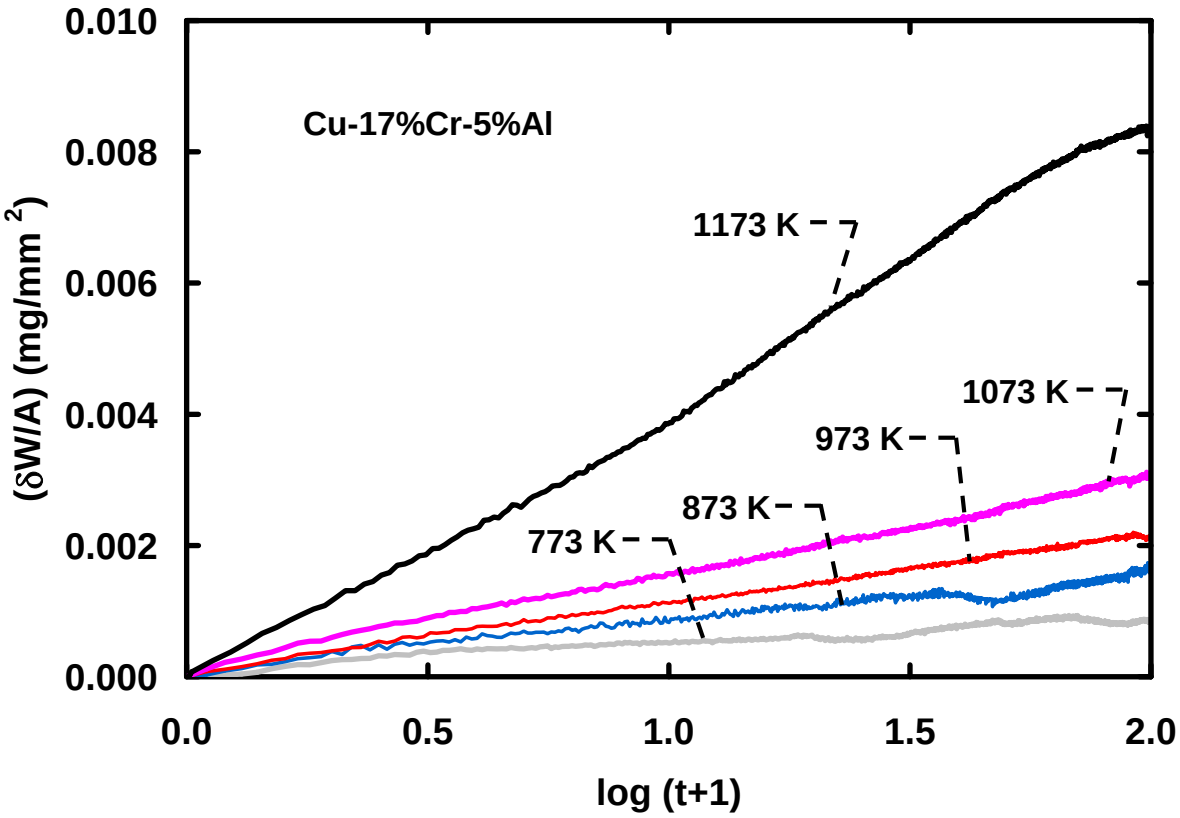

Fig. 10 Plot of the specific weight change against log (t+1) demonstrating the applicability of the direct logarithmic relationship to describe the oxidation behavior of Cu-17%Cr-5%Al.

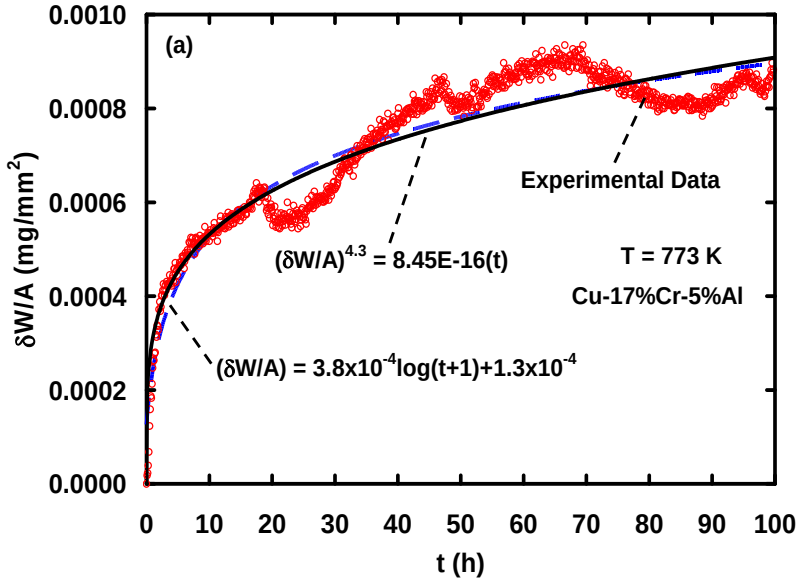
(a)
δW/A (mg/mm²)
t (h)
(δW/A)^4.3 = 8.45E-16(t)
(δW/A) = 3.8x10^-4 log(t+1)+1.3x10^-4
Experimental Data
T = 773 K
Cu-17%Cr-5%Al

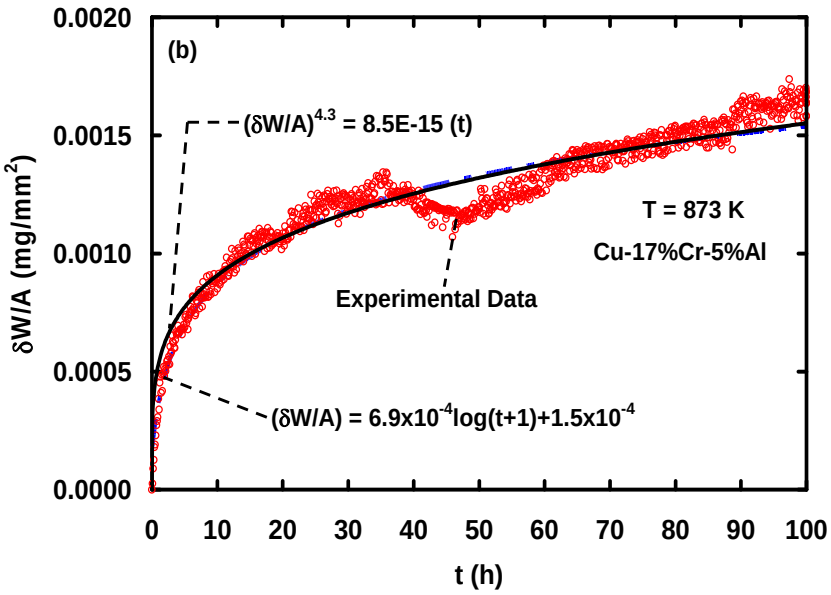
(b)
δW/A (mg/mm²)
t (h)
(δW/A)^4.3 = 8.5E-15 (t)
(δW/A) = 6.9x10^-4 log(t+1)+1.5x10^-4
Experimental Data
T = 873 K
Cu-17%Cr-5%Al

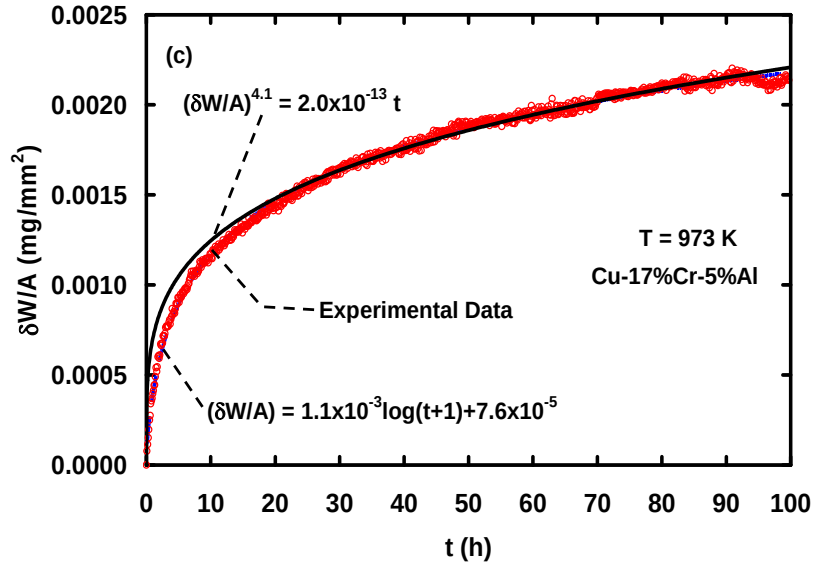
(c)
δW/A (mg/mm²)
t (h)
(δW/A)^4.1 = 2.0x10^-13 t
(δW/A) = 1.1x10^-3 log(t+1)+7.6x10^-5
Experimental Data
T = 973 K
Cu-17%Cr-5%Al

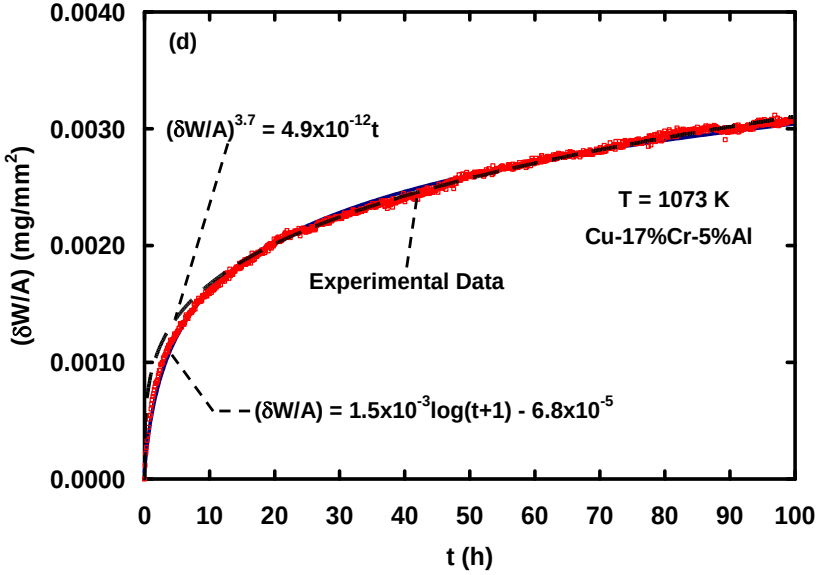
(d)
(δW/A) (mg/mm²)
t (h)
(δW/A)^3.7 = 4.9x10^-12 t
(δW/A) = 1.5x10^-3 log(t+1) - 6.8x10^-5
Experimental Data
T = 1073 K
Cu-17%Cr-5%Al

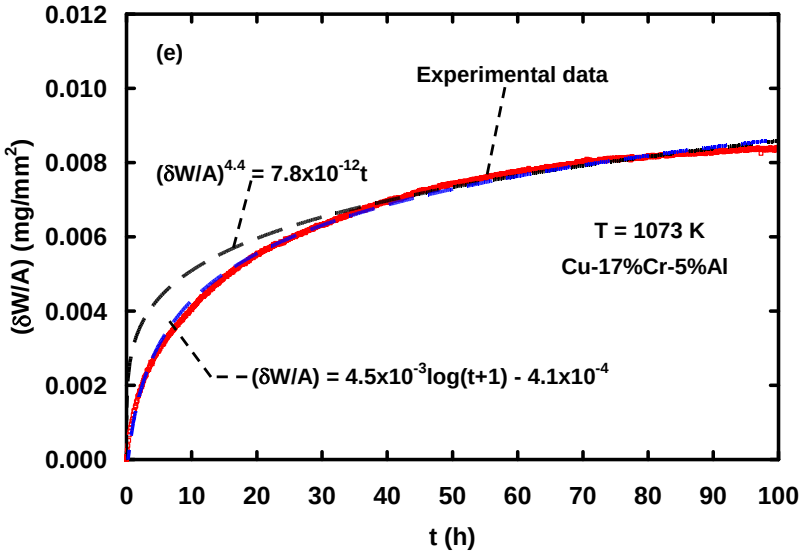

Fig. 11 Comparison of the logarithmic and quartic regression equations with the experimental data for Cu-17%Cr-5%Al. (a) 773 K; (b) 873 K; (c) 973 K; (d) 1073 K; (e) 1173 K.

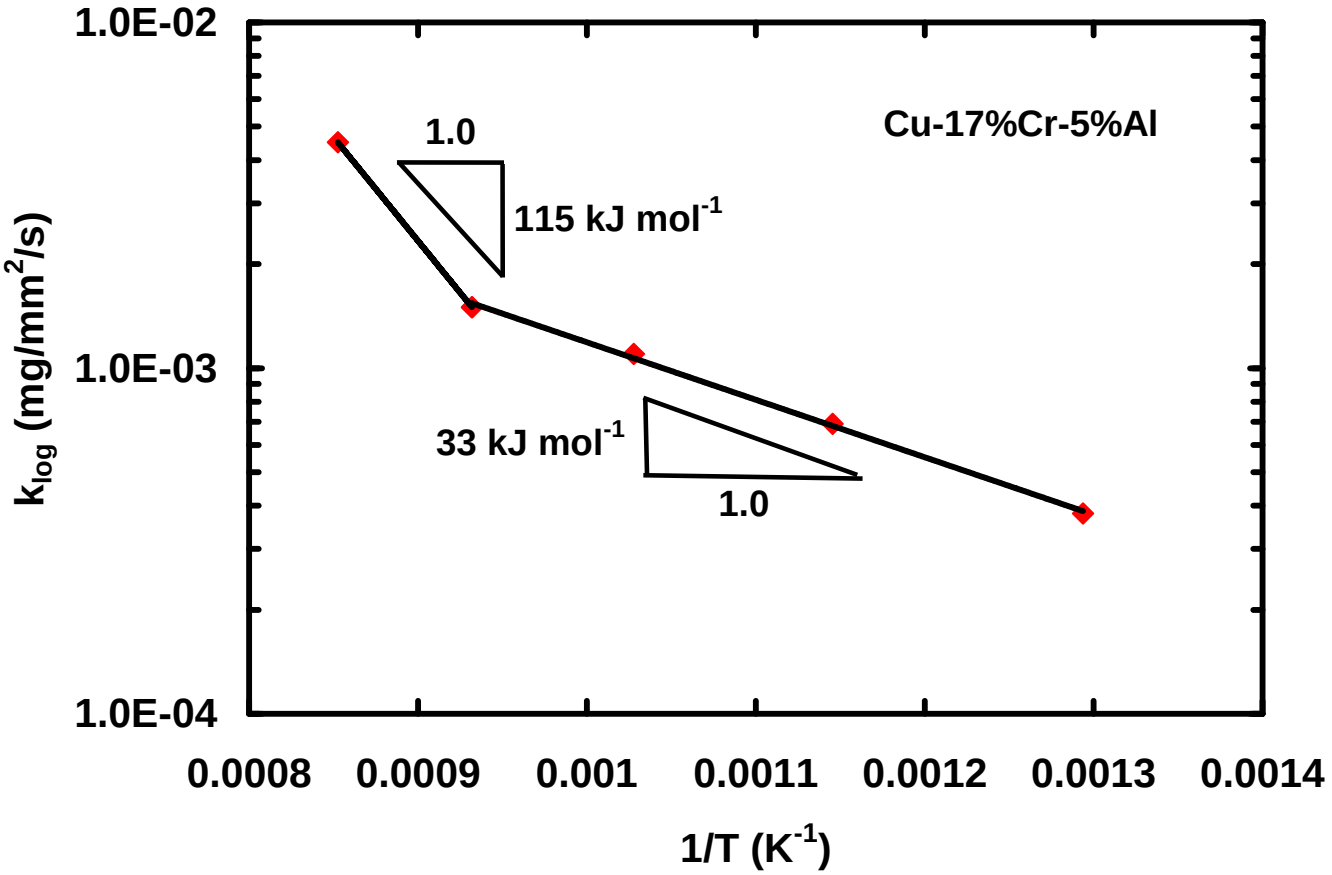

Fig. 12 Arrhenius plot of the logarithmic rate constant against the inverse of the absolute temperature for Cu-17%Cr-5%Al.